Geology

Enhanced carbon dioxide outgassing from the eastern equatorial Atlantic during the last glacial

G.L. Foster and P.F. Sexton

Geology published online 7 October 2014;
doi: 10.1130/G35806.1

Notes

Geology, published online on 7 October 2014 as doi:10.1130/G35806.1

Enhanced carbon dioxide outgassing from the eastern equatorial Atlantic during the last glacial

G.L. Foster[1]* and P.F. Sexton[2]

[1]Ocean and Earth Science, National Oceanography Centre, Southampton, University of Southampton, Waterfront Campus, Southampton SO14 3ZH, UK

[2]Centre for Earth, Planetary, Space and Astronomical Research, The Open University, Walton Hall, Milton Keynes MK7 6AA, UK

ABSTRACT

Biological productivity and carbon export in the equatorial Atlantic are thought to have been dramatically higher during the last glacial period than during the Holocene. Here we reconstruct the pH and CO_2 content of surface waters from the eastern equatorial Atlantic Ocean over the past ~30 k.y. using the boron isotope composition of *Globigerinoides ruber* (a mixed-layer–dwelling planktic foraminifera). Our new record, combined with previously published data, indicates that during the last glacial, in contrast to today, a strong west to east gradient existed in the extent of air:sea equilibrium with respect to pCO_2 (ΔpCO_2), with the eastern equatorial Atlantic acting as a significant source of CO_2 (+100 µatm) while the western Atlantic remained close to equilibrium (+25 µatm). This pattern suggests that a five-fold increase in the upwelling rate of deeper waters drove increased Atlantic productivity and large-scale regional cooling during the last glacial, but the higher than modern ΔpCO_2 in the east indicates that export production did not keep up with enhanced upwelling of nutrients. However, the downstream decline of ΔpCO_2 provides evidence that the unused nutrients from the east were eventually used for biologic carbon export, thereby effectively negating the impact of changes in upwelling on atmospheric CO_2 levels. Our findings indicate that the equatorial Atlantic exerted a minimal role in contributing to lower glacial-age atmospheric CO_2.

INTRODUCTION

Over at least the past 800 k.y., the CO_2 content of the atmosphere has shifted from ~240–280 ppm during the warm interglacial periods to 180–200 ppm during the cold glacial periods (Petit et al., 1999; Lüthi et al., 2008); most attention has been focused on the amount of carbon stored in the deep ocean during glacials to explain these CO_2 changes (e.g., Sigman et al., 2010). One important mechanism in this regard is the biological pump: biomass produced in the surface ocean sinks to depth and decomposes, thereby pumping both nutrients and organic carbon into the deep ocean, where the carbon is sequestered away from the atmosphere and the nutrients are temporarily unavailable to fuel new biological production. Given their importance today in terms of oceanic primary production (Fig. 1B), attention has long focused on the equatorial oceans to at least partially explain the lower glacial CO_2 levels (e.g., Mix, 1989).

A small proportion of the equatorial regions is termed high-nitrate, low-chlorophyll (HNLC; e.g., the eastern equatorial Pacific Ocean), where the plentiful supply of macronutrients (N, P) from upwelling of cold (Fig. 1A), nutrient-rich (Fig. 1C) and high-CO_2 (Fig. 1D) water is often underutilized because of the relative paucity of essential micronutrients such as Fe (Moore et al., 2013). The incomplete utilization of macronutrients in HNLC regions gives rise to outgassing of excess CO_2 to the atmosphere (Fig. 1D). Changing the efficiency of nutrient utilization (e.g., through enhanced productivity via dust fertilization of Fe-limited areas; Martin, 1990) clearly has the potential to lower the pCO_2^{sw} (sw is seawater) in these regions. However, most areas of the equatorial and low-latitude oceans are non-HNLC regions, where productivity is not micronutrient limited (e.g., by Fe), and organisms are eventually able to fully utilize all the available macronutrients (N, P; Fig. 1C) with correspondingly lower quantities (5–30 µatm) of excess CO_2 (defined herein as $\Delta pCO_2 = pCO_2^{sw} - pCO_2^{atm}$; e.g., the eastern equatorial Atlantic; Fig. 1D). As a result, across the low-latitude non-HNLC regions macronutrient (as opposed to micronutrient) limitation currently exists (Moore et al., 2013). In these regions, there is more limited scope to decrease pCO_2^{sw} by enhanced nutrient utilization, since most of the nutrients are already nearly fully utilized.

Despite the apparent potential for changing pCO_2^{sw} in either HNLC or non-HNLC regions via alleviation of macronutrient or micronutrient limitation, it has been hypothesized that their role in glacial-interglacial CO_2 change should have been minor (Sigman et al., 2010; Hain et al., 2014), because of the following:

(1) Nutrients supplied to the low-latitude surface from below are all eventually consumed by productivity as the nutrient-rich water flows away from the site of upwelling before the water is able to sink into the ocean interior (Sigman and Haug, 2003). Even if an increase in on-axis (where axis refers to the longitudinally extensive zone of upwelling) consumption of nutrients occurred in an equatorial upwelling region (e.g., due to a relief from Fe limitation), leading to a local decrease in pCO_2^{sw}, this may not change atmospheric CO_2 significantly because off-axis productivity may be correspondingly reduced, causing little net change in the residual unused nutrient concentration when the water ultimately descends back into the ocean interior. This almost complete utilization of available nutrients is in stark contrast to higher latitudes, such as the Southern Ocean, where the utilization of nutrients is currently inefficient (and consequently is associated with outgassing of CO_2), but may have been more efficient during glacial times (e.g., Sigman et al., 2010).

(2) The high-latitude surface ocean is in direct communication with the deep ocean, whereas the low-latitude surface ocean is not, so changes in low-latitude pCO_2^{sw} are hypothesized to be somewhat buffered from driving atmospheric CO_2 changes because of the much larger size of the high-latitude/deep-ocean reservoir (Broecker et al., 1999).

One region of the oceans that has well-documented changes in surface ocean productivity and export production across glacial-interglacial cycles is the equatorial Atlantic (Bradtmiller et al., 2007; Kohfeld et al., 2005, and references therein, and their figure 2c). While this has been interpreted as evidence of a strengthening of the biological pump and hence driving a portion of glacial CO_2 drawdown (e.g., Mix, 1989), this remains to be quantitatively tested. Here we use the boron isotopic composition (expressed in terms of $\delta^{11}B$) of mixed-layer-dwelling planktic foraminifera *Globigerinoides ruber* to reconstruct surface water pH and therefore pCO_2^{sw} across a transect of sites spanning the equatorial Atlantic Ocean over the past ~30 k.y., allowing us to directly test the role of this region in glacial-interglacial pCO_2^{atm} variations.

METHODOLOGY

Samples from ca. 30 ka to 10 ka were selected from Site GeoB1105-4 (R/V *Meteor* cruise M9/4; herein GeoB1105) from the eastern equatorial Atlantic (Fig. 1), located near the center of modern upwelling. Age models for the studied period were discussed by Henehan et al. (2013) for Ocean Drilling Program (ODP) Site 999 and Site GeoB1523, and based on ^{14}C dating for GeoB1105 (Bickert and Mackensen, 2003). Our new data, combined with published $\delta^{11}B$ data for *G. ruber* from ODP Site 999A

*E-mail: gavin.foster@noc.soton.ac.uk.

Data Repository item 2014351 | doi:10.1130/G35806.1

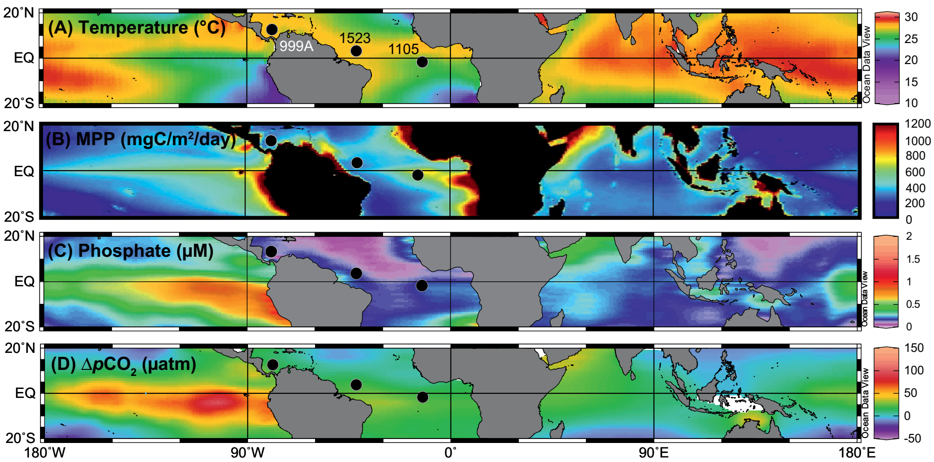

Figure 1. Surface water of the modern equatorial Atlantic, Indian, and Pacific Oceans constructed using Ocean Data View software (R. Schlitzer, 2014, http://odv.awi.de). EQ—equator. A: Mean annual sea-surface temperature (Locarnini et al., 2006). Sites used in this study are shown (see text). B: Mean primary productivity (MPP). Data were derived from satellite data available at http://oceancolor.gsfc.nasa.gov and http://pathfinder.nodc.noaa.gov/ using the vertically generalized productivity model of Behrenfeld and Falkowski (1997). C: Mean annual phosphate (Garcia et al., 2006). D: Mean annual ΔpCO_2 (Takahashi et al., 2009). Note that ΔpCO_2 in eastern equatorial Atlantic during some seasons can locally be 80–100 µatm (Bakker et al., 2001).

(herein ODP 999) and Site GeoB1523-1 (herein GeoB1523) from the Caribbean and western equatorial Atlantic, respectively (Foster, 2008; Henehan et al., 2013), allow us to examine zonal gradients in surface ocean carbonate chemistry (Fig. 1). All boron isotopic measurements presented here were performed by multicollector–inductively coupled plasma–mass spectrometry at the University of Bristol (UK), closely following the methodologies in Foster (2008) and Rae et al. (2011). The basis for the boron isotope-pH proxy was discussed extensively elsewhere (e.g., Foster, 2008; Rae et al., 2011), and we use the new δ^{11}B-pH calibration for this species (Henehan et al., 2013). We also generated sea-surface temperature (SST) records for the same samples using Mg/Ca ratio of *G. ruber* and the calibration of Anand et al. (2003). See the GSA Data Repository[1] for more details of the methodologies used to calculate pH and pCO_2^{sw} from δ^{11}B; the relevant data are in Table DR1.

RESULTS

Figure 2 shows data from the three sites in the eastern Atlantic Ocean (blue), western Atlantic (black), and Caribbean (red). Our Mg/Ca-derived SST records reveal a persistent pattern throughout the past 30 k.y. of an eastward decrease in SST (i.e., $SST_{999A} > SST_{GeoB1523} > SST_{GeoB1105}$; Fig. 2), but with larger differences between the sites before ca. 18 ka and the greatest extent of glacial-aged cooling at our easternmost site (GeoB1105; Fig. 2A). δ^{11}B values of *G. ruber* and the calculated surface-water pH exhibit similar values across the three sites during Marine Isotope Stage 1 (MIS 1; Figs. 2B and 2C), consistent with the absence of a major pH gradient in the Atlantic today. However, δ^{11}B and calculated pH diverge during MIS 2 (Figs. 2B and 2C). From these δ^{11}B and pH records, we calculate that surface water in the Caribbean and western Atlantic (ODP 999 and GeoB1523) remained close to equilibrium with the atmosphere (purple line in Fig. 2D) with respect to CO_2 for the past 30 k.y., albeit with a minor and consistent offset comparable to that observed today at both sites (20–30 µatm; Figs. 1D and 2D). This contrasts with GeoB1105 in the eastern equatorial Atlantic, where we reconstruct a significant excess of pCO_2^{sw} compared to the contemporaneous atmosphere (by >100 µatm), indicating that this region was a strong source of CO_2 to the atmosphere during MIS 2 and MIS 3. Therefore, in marked contrast to MIS 1 (Fig. 2), a significant east to west gradient in ΔpCO_2 existed during the last glacial that was well correlated with the contemporaneous SST gradient (Figs. 2, 3A, and 3B). Notably, this strong cross-basin gradient in calculated pCO_2^{sw} is also evident in δ^{11}B alone, as reflected in the large differences between δ^{11}B of *G. ruber* (to 1.5‰) from the three sites during the last glacial (e.g., ODP 999 versus GeoB1105; Fig. 2B) in comparison to correspondingly small δ^{11}B gradients during MIS 1.

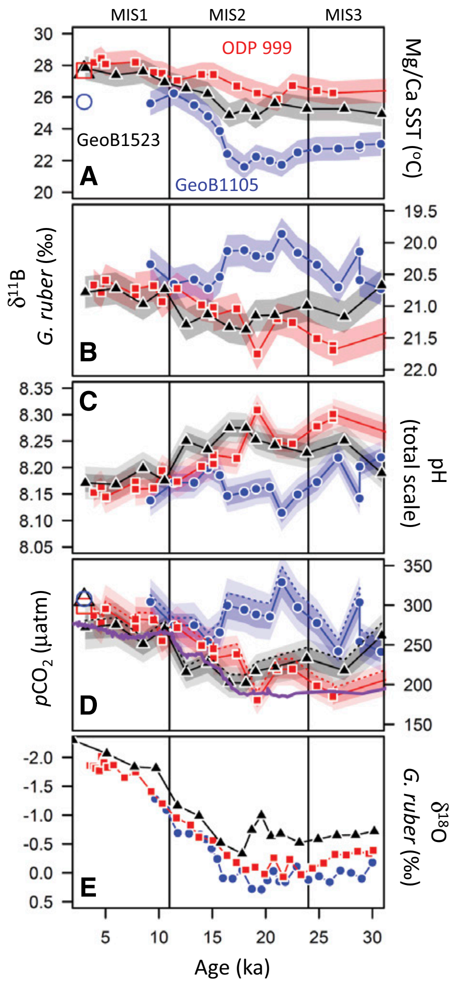

Figure 2. Data from three sites in the eastern Atlantic Ocean. Ocean Drilling Program (ODP) Site 999 is shown by red squares, Site GeoB1523 (R/V *Meteor* cruise M16/2), is shown by black triangles, and Site GeoB1105 (R/V *Meteor* cruise M9/4) is shown by blue circles; vertical lines denote the boundaries for the marine isotope stages. A: Mg/Ca based sea-surface temperature (SST, with 1σ uncertainty band ±0.75 °C); modern SSTs for each site are shown as open colored symbols. B: δ^{11}B for *Globigerinoides ruber* with analytical uncertainty shown as a band (±0.25‰; 2σ). C: Mixed-layer pH (error band is ±1σ as dark band, ±2σ as light band). D: pCO_2^{sw} (sw—seawater) calculated using an assumed constant total alkalinity of 2300 µmol/kg (solid line); error band is as for pH. Dotted lines are pCO_2^{sw} calculated using a total alkalinity that scales with salinity (for more details, see the Data Repository [see footnote 1]). Modern pCO_2^{sw} at these locations (from Takahashi et al., 2009) are shown as open colored symbols. Purple line is atmospheric CO_2 from ice cores (Monnin et al., 2001; Petit et al., 1999). E: δ^{18}O for *G. ruber* from Schmidt et al. (2004), Schneider et al. (1996), and Mulitza et al. (1998) for ODP Site 999, Site GeoB1523, and Site GeoB1105, respectively.

[1]GSA Data Repository item 2014351, data table, details of methods, and a figure showing phosphate concentration over the past 30 k.y. at GeoB1105, is available online at www.geosociety.org/pubs/ft2014.htm, or on request from editing@geosociety.org or Documents Secretary, GSA, P.O. Box 9140, Boulder, CO 80301, USA.

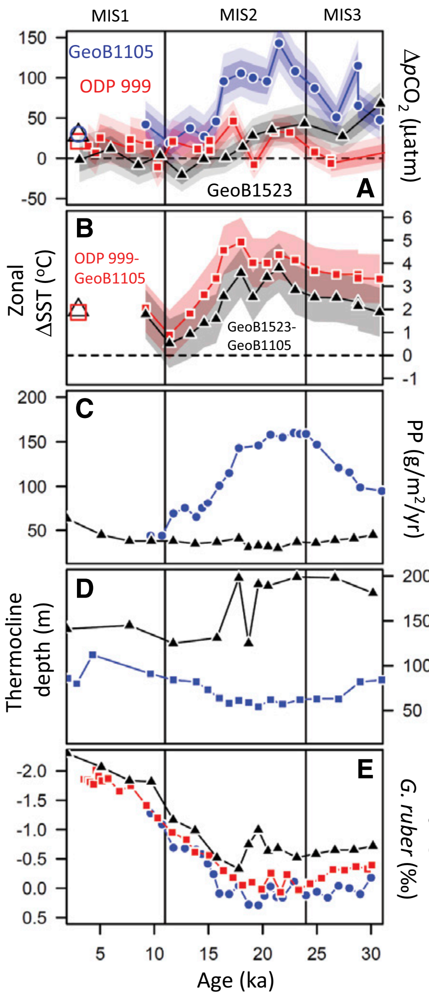

Figure 3. Data from three sites in the eastern Atlantic Ocean. Ocean Drilling Program (ODP) Site 999 is shown in red, Site GeoB1523 (R/V *Meteor* cruise M16/2), is shown in black, and Site GeoB1105 (R/V *Meteor* cruise M9/4) is shown in blue; vertical lines denote the boundaries for the marine isotope stages. A: Boron isotope-derived ΔpCO_2 (sea-air) for Ocean Drilling Program (ODP) Site 999, Site GeoB1105, and Site GeoB1523. Modern mean annual disequilibrium is shown as open symbols (ODP 999 = +21 µatm, GeoB1523 = +29 µatm, GeoB1105 = +30 µatm). B: Zonal sea-surface temperature (ΔSST) gradient between Sites GeoB1105 and ODP 999 (red) and GeoB1105 and GeoB1523 (black). Error band is a quadratic addition of 1σ uncertainty (±0.75 °C) for each record; modern SST gradient is shown by open symbols. C: Paleo–primary productivity (PP; as g/m²/yr of carbon export) for GeoB1105 (Schmidt et al., 2003) and GeoB1523 (Rühlemann et al., 1996). D: Thermocline depth from foraminiferal transfer functions for GeoB1523 and GeoB1105 (Wolff et al., 1999). E: $\delta^{18}O$ for *Globigerinoides ruber* from Schmidt et al. (2004), Schneider et al. (1996), and Mulitza et al. (1998) for Sites ODP 999, GeoB1523, and GeoB1105, respectively.

DISCUSSION

Our SST reconstruction across the equatorial Atlantic (Fig. 2A) shows a glacial-age cooling that was stronger in the east (3–4 °C) than the west (1–2 °C) (e.g., MARGO Project Members, 2009; Pflaumann et al., 2003), likely attributable to enhanced eastern upwelling of cold water owing to stronger glacial-age southeast trade winds (Mix and Morey, 1996; Wolff et al., 1999; MARGO Project Members, 2009). Intensified glacial upwelling in the east is also consistent with an increased east to west tilt in the equatorial Atlantic thermocline (Fig. 3D; Wolff et al., 1999), a shallow nutricline in the east (Molfino and McIntyre, 1990), and a consequent increase in primary productivity (Fig. 3C; Schmidt et al., 2003) and opal fluxes (not shown; Bradtmiller et al., 2007), and an increase in ΔpCO_2 (Fig. 3A) at eastern Site GeoB1105.

In the eastern equatorial Atlantic today, during a particularly strong upwelling season, SSTs cool considerably and ΔpCO_2 can locally reach as high as 80–100 µatm at 12°W (Bakker et al., 2001), compared to 25–50 µatm during other years in the climatology of Takahashi et al. (2009) (Fig. 1D). The simplest explanation of our reconstructions for the past 30 k.y. is that, during the last glacial, the upwelling of cold, CO_2-rich water with significant CO_2 excess compared to the atmosphere was the norm in the eastern Atlantic, rather than the exception. In the modern ocean, only those regions where nutrient utilization is inefficient (due to micronutrient limitation) are significant sources of CO_2 to the atmosphere (Fig. 1D). A number of reconstructions indicate that the dust-related Fe flux to the eastern equatorial Atlantic during MIS 2 and 3 was likely even higher than today (by 2–5× ; Kohfeld and Harrison, 2001; Bradtmiller et al., 2007; Mahowald et al., 1999). In addition, diatom productivity increased throughout the equatorial Atlantic, suggesting an enhanced Si supply, probably from Southern Ocean sources (Bradtmiller et al., 2007). It is therefore very unlikely that the strong CO_2 outgassing in the eastern equatorial Atlantic that we have shown during MIS 2 and 3 was due to micronutrient (Fe) or Si limitation (as in the modern eastern equatorial Pacific). Instead, it is probable that the strength of upwelling was sufficiently high to overwhelm the observed increase in productivity to maintain elevated surface nutrient (and pCO_2^{sw}) levels, as happens today during strong upwelling seasons (Bakker et al., 2001). Given the excess CO_2 (associated with the reconstructed ΔpCO_2^{sw}) at GeoB1105 and the $\delta^{13}C$ gradient between ODP 999 and GeoB1105, we calculate a glacial age (between 18 and 25 ka) surface water $[PO_4^{3-}]$ of ~0.7 µM at GeoB1105, comparable to the eastern equatorial Pacific today (Fig. 1D; for details of this calculation, see the Data Repository). If the $[PO_4^{3-}]$ of the thermocline was similar to today (~1.5 µM), and given the threefold increase in primary production (Schmidt et al., 2003), this estimate of surface water $[PO_4^{3-}]$ suggests a fivefold increase in the rate of upwelling (for full details, see the Data Repository). Because the $[PO_4^{3-}]$ of deep water upwelled in the eastern Atlantic during the last glacial likely decreased (due to the dominance of Glacial North Atlantic Intermediate Water at mid-depth; Straub et al., 2013), this is likely to be a minimum estimate.

As the CO_2-rich surface waters in the east were advected westward during the last glacial toward the western (GeoB1523) equatorial Atlantic and Caribbean (ODP 999), ΔpCO_2 rapidly decreased (to ~20–30 µatm; Fig. 3A), probably through biological utilization of CO_2, as in the modern equatorial Pacific (Quay, 1997). While primary productivity at GeoB1523 was not higher during MIS 2 (Fig. 3C), it is apparent from the regional compilations of Kohfeld et al. (2005) and Bradtmiller et al. (2007) that export production was enhanced throughout much of the eastern and western equatorial Atlantic (Bradtmiller et al., 2007, their figure 2c). We therefore conclude that the enhanced biological productivity in the equatorial Atlantic during the last glacial (e.g., 3× higher rates of C_{org} burial and primary productivity during MIS 2 compared to MIS 1; Fig. 3C) was primarily driven by enhanced upwelling in the eastern part of the basin (e.g., Schmidt et al., 2003) and the lateral transport of unused nutrient from the site of enhanced upwelling (and incomplete nutrient consumption) toward the central and western equatorial Atlantic. Our data from the eastern Atlantic demonstrate that this enhanced upwelling (and the presumed incomplete consumption of nutrients) increased the excess CO_2 in the eastern Atlantic surface, thereby enhancing local CO_2 outgassing. However, by analogy with the modern Pacific equatorial upwelling system, our data from the western equatorial Atlantic and Caribbean (Fig. 3A) suggest that the excess CO_2 upwelled in the east was ultimately consumed by intensified downstream biological carbon export, fuelled by the unused nutrients that were laterally advected alongside the excess CO_2. For this reason, the coupled intensification of upwelling in the east and a stronger biological pump in the wider equatorial Atlantic region likely had little or no effect on glacial atmospheric CO_2 levels.

CONCLUSIONS

By reconstructing the patterns of pCO_2^{sw} across the equatorial Atlantic over the past 30 k.y. we demonstrate that the equatorial Atlantic underwent an at least fivefold increase in the rate of upwelling. Although this upwelling intensified regional productivity (Kohfeld et al., 2005; Schmidt et al., 2003), our reconstructed higher than modern ΔpCO_2 for the eastern equatorial Atlantic indicates that export production did not keep pace with the strengthened upwelling of nutrients, giving rise to significant CO_2 outgassing (Fig. 3A). We thus find that the low-latitude Atlantic was not a significant contributor to the drawdown of atmospheric CO_2 concentrations during the last glacial, providing support for the dominance of high-latitude processes in glacial-interglacial CO_2 change.

ACKNOWLEDGMENTS

This work was supported by Natural Environment Research Council (NERC) grant NE/D00876X/2 to Foster and NERC grant NE/I006346/1 to Sexton and Foster. We thank Chris Coath for maintaining the mass spectrometers at the University of Bristol (UK) and James Rae and Mathis Hain for discussion on an earlier draft of this manuscript. We also thank Stephanie Henson for producing panel B of Figure 1, Barbara Donner for supplying samples from Site GeoB1105, and Karen Kohfeld, Jimin Yu, and two anonymous reviewers for thorough reviews that significantly improved the manuscript.

REFERENCES CITED

Anand, P., Elderfield, H., and Conte, M., 2003, Calibration of Mg/Ca thermometry in planktonic foraminifera from a sediment trap time series: Paleoceanography, v. 18, doi:10.1029/2002PA000846.

Bakker, D.C.E., Etcheto, J., Boutin, J., and Merlivat, L., 2001, Variability of surface water f_{CO2} during seasonal upwelling in the equatorial Atlantic Ocean as observed by a drifting buoy: Journal of Geophysical Research, v. 106, p. 9241–9253, doi:10.1029/1999JC000275.

Behrenfeld, M.J., and Falkowski, P.G., 1997, Photosynthetic rates derived from satellite-based chlorophyll concentration: Limnology and Oceanography, v. 42, p. 1–20, doi:10.4319/lo.1997.42.1.0001.

Bickert, T., and Mackensen, A., 2003, Last glacial to Holocene changes in South Atlantic Deep Water circulation, *in* Wefer, G., et al., eds., The South Atlantic in the late Quaternary: Reconstruction of material budgets and current systems: Berlin, Heidelberg, Springer-Verlag, p. 671–695.

Bradtmiller, L.I., Anderson, R.F., Fleisher, M.Q., and Burckle, L., 2007, Opal burial in the equatorial Atlantic Ocean over the last 30 ka: Implications for glacial-interglacial changes in the ocean silicon cycle: Paleoceanography, v. 22, doi:10.1029/2007PA001443.

Broecker, W.S., Lynch-Steiglitz, J., Archer, D., Hofmann, M., Maier-Reimer, E., Marchal, O., Stocker, T., and Gruber, N., 1999, How strong is the Havardton-Bear constraint?: Global Biogeochemical Cycles, v. 13, p. 817–820, doi:10.1029/1999GB900050.

Foster, G.L., 2008, Seawater pH, pCO_2 and $[CO_3^{2-}]$ variations in the Caribbean Sea over the last 130 kyr: A boron isotope and B/Ca study of planktic foraminifera: Earth and Planetary Science Letters, v. 271, p. 254–266, doi:10.1016/j.epsl.2008.04.015.

Garcia, H.E., Locarnini, R.A., Boyer, T.P., and Antonov, J.I., 2006, World ocean atlas, Volume 4: Nutrients (phosphate, nitrate, silicate): NOAA Atlas NESDIS 71: Washington, D.C., U.S. Government Printing Office, 396 p.

Hain, M.P., Sigman, D.M., and Haug, G.J., 2014, The biological pump in the past, *in* Holland, H.D., and Turekian, K.K., eds., Treatise on geochemistry (second edition): Oxford, UK, Elsevier, p. 485–517.

Henehan, M.J., et al., 2013, Calibration of the boron isotope proxy in the planktonic foraminifera *Globigerinoides ruber* for use in palaeo-CO_2 reconstruction: Earth and Planetary Science Letters, v. 364, p. 111–122, doi:10.1016/j.epsl.2012.12.029.

Kohfeld, K.E., and Harrison, S.P., 2001, DIRTMAP: The geological record of dust: Earth-Science Reviews, v. 54, p. 81–114, doi:10.1016/S0012-8252(01)00042-3.

Kohfeld, K.E., Le Quere, C., Harrison, S.P., and Anderson, R.F., 2005, Role of marine biology in glacial-interglacial CO_2 cycles: Science, v. 308, p. 74–78, doi:10.1126/science.1105375.

Locarnini, R.A., Mishonov, A.V., Antonov, J.I., Boyer, T.P., and Garcia, H.E., 2006, World Ocean Atlas 2005, Volume 1: Temperature: NOAA Atlas NESDIS 68: Washington, D.C., U.S. Government Printing Office, 182 p.

Lüthi, D., et al., 2008, High-resolution carbon dioxide concentration record 650,000–800,000 years before present: Nature, v. 453, p. 379–382, doi:10.1038/nature06949.

Mahowald, N., Kohfeld, K.E., Hansson, M., Balkanski, Y., Harrison, S.P., Prentice, I.C., Schulz, M., and Rodhe, H., 1999, Dust sources and deposition during the last glacial maximum and current climate: A comparison of model results with paleodata from ice cores and marine sediments: Journal of Geophysical Research, v. 104, p. 15895–15916, doi:10.1029/1999JD900084.

MARGO Project Members, 2009, Constraints on the magnitude and patterns of ocean cooling at the Last Glacial Maximum: Nature Geoscience, v. 2, p. 127–132, doi:10.1038/ngeo411.

Martin, J., 1990, Glacial-interglacial CO_2 change: The iron hypothesis: Paleoceanography, v. 5, p. 1–13, doi:10.1029/PA005i001p00001.

Mix, A.C., 1989, Influence of productivity variations on long-term atmospheric CO_2: Nature, v. 337, p. 541–544, doi:10.1038/337541a0.

Mix, A.C., and Morey, A.E., 1996, Climate feedback and Pleistocene variations in the Atlantic South Equatorial current, *in* Wefer, G., et al., eds., The South Atlantic: Present and past circulation: Berlin, Heidelberg, Springer-Verlag, p. 503–525.

Molfino, B., and McIntyre, A., 1990, Precessional forcing of nutricline dynamics in the equatorial Atlantic: Science, v. 249, p. 766–769, doi:10.1126/science.249.4970.766.

Monnin, E., Indermühle, A., Dällenbach, A., Flückiger, J., Stauffer, B., Stocker, T.F., Raynaud, D., and Barnola, J.-M., 2001, Atmospheric CO_2 concentrations over the last glacial termination: Science, v. 291, p. 112–114, doi:10.1126/science.291.5501.112.

Moore, C.M., et al., 2013, Processes and patterns of oceanic nutrient limitation: Nature Geoscience, v. 6, p. 701–710, doi:10.1038/ngeo1765.

Mulitza, S., Rühlemann, C., Bickert, T., Hale, W., Pätzold, J., and Wefer, G., 1998, Late Quaternary $\delta^{13}C$ gradients and carbonate accumulation in the western equatorial Atlantic: Earth and Planetary Science Letters, v. 155, p. 237–249, doi:10.1016/S0012-821X(98)00012-0.

Petit, J.R., et al., 1999, Climate and atmospheric history of the past 420,000 years from the Vostok ice core, Antarctica: Nature, v. 399, p. 429–436, doi:10.1038/20859.

Pflaumann, U., et al., 2003, Glacial North Atlantic: Sea-surface conditions reconstructed by GLAMAP 2000: Paleoceanography, v. 18, 1065, doi:10.1029/2002PA000774.

Quay, P., 1997, Was a carbon balance measured in the equatorial Pacific during JGOFS?: Deep-Sea Research. Part II, v. 44, p. 1765–1781, doi:10.1016/S0967-0645(97)00093-3.

Rae, J.W.B., Foster, G.L., Schmidt, D.N., and Elliott, T., 2011, Boron isotopes and B/Ca in benthic foraminifera: Proxies for the deep ocean carbonate system: Earth and Planetary Science Letters, v. 302, p. 403–413, doi:10.1016/j.epsl.2010.12.034.

Rühlemann, C., Frank, M., Hale, W., Mangini, A., Mulitza, S., Müller, P.J., and Wefer, G., 1996, Late Quaternary productivity changes in the western equatorial Atlantic: Evidence from ^{230}Th-normalized carbonate and organic carbon accumulation rates: Marine Geology, v. 135, p. 127–152, doi:10.1016/S0025-3227(96)00048-5.

Schmidt, D.N., Renaud, S., and Bollmann, J., 2003, Response of planktic foraminiferal size to late Quaternary climate change: Paleoceanography, v. 18, 1039, doi:10.1029/2002PA000831.

Schmidt, M.W., Spero, H.J., and Lea, D.W., 2004, Links between salinity variation in the Caribbean and North Atlantic thermohaline circulation: Nature, v. 428, p. 160–163, doi:10.1038/nature02346.

Schneider, R.R., Müller, P.J., Ruhland, G., Meineke, G., Schmidt, H., and Wefer, G., 1996, Late Quaternary surface temperatures and productivity in the East-Equatorial South Atlantic: Response to changes in trade/monsoon wind forcing and surface water advection, *in* Wefer, G., et al., eds., The South Atlantic: Present and past circulation: Berlin, Heidelberg, Springer-Verlag, p. 527–551.

Sigman, D.M., and Haug, G.H., 2003, The biological pump in the past, *in* Elderfield, E., ed., The oceans and marine geochemistry: Treatise on geochemistry Volume 6: Oxford, UK, Elsevier-Pergamon, p. 491–528, doi:10.1016/B978-0-08-095975-7.00618-5.

Sigman, D.M., Hain, M.P., and Haug, G.H., 2010, The polar ocean and glacial cycles in atmospheric CO_2 concentration: Nature, v. 466, p. 47–55, doi:10.1038/nature09149.

Straub, M., Sigman, D.M., Ren, H., Martinez-Garcia, A., Meckler, A.N., Hain, M.P., and Haug, G.H., 2013, Changes in North Atlantic nitrogen fixation controlled by ocean circulation: Nature, v. 501, p. 200–203, doi:10.1038/nature12397.

Takahashi, K., et al., 2009, Climatological mean and decadal change in surface ocean pCO_2, and net sea-air CO_2 flux over the global oceans: Deep-Sea Research, Part II, v. 56, p. 554–577, doi:10.1016/j.dsr2.2008.12.009.

Wolff, T., Mulitza, S., Rühlemann, C., and Wefer, G., 1999, Response of the tropical Atlantic thermocline to late Quaternary trade wind changes: Paleoceanography, v. 14, p. 374–383, doi:10.1029/1999PA900011.

Manuscript received 25 April 2014
Revised manuscript received 14 August 2014
Manuscript accepted 14 August 2014

Printed in USA